Vapor flows condensing at incidence onto a plane condensed phase in the presence of a noncondensable gas. II. Supersonic condensation

Satoshi Taguchi, Kazuo Aoki,[a] and Shigeru Takata
Department of Aeronautics and Astronautics, Graduate School of Engineering, Kyoto University, Kyoto 606-8501, Japan

(Received 24 July 2003; accepted 8 October 2003; published online 3 December 2003)

This paper is the second part of the study of a steady flow of a vapor in a half space condensing onto a plane condensed phase of the vapor at incidence in the presence of a noncondensable gas near the condensed phase. The aim of the study is to clarify the behavior of the vapor and noncondensable gas on the basis of kinetic theory under the assumption that the molecules of the noncondensable gas are mechanically identical with those of the vapor. In the first part [S. Taguchi *et al.*, Phys. Fluids **15**, 689 (2003)], the case of subsonic condensation, where the Mach number corresponding to the flow-velocity component perpendicular to the condensed phase at infinity is less than unity, is considered. In the present second part, the case of supersonic condensation is investigated in detail on the same lines as the first part. © *2004 American Institute of Physics.*
[DOI: 10.1063/1.1630324]

I. INTRODUCTION

We consider a steady flow of a vapor in a half space condensing onto a plane condensed phase of the vapor at incidence in the case where another gas that does not condense (the noncondensable gas) is present near the condensed phase. We investigate the behavior of the vapor as well as the noncondensable gas on the basis of kinetic theory. Our main interest is to obtain the relation, among the parameters of the vapor at infinity (the pressure, temperature, and flow velocity of the vapor), those related to the condensed phase (the temperature of the condensed phase and the corresponding saturation pressure of the vapor), and the amount of the noncondensable gas contained in the system, that admits a steady solution.

This problem was investigated in detail in Ref. 1, where the case in which the vapor condenses perpendicularly to the condensed phase was considered. The essential point of Ref. 1 is a skillful analysis, based on the assumption that the noncondensable-gas molecules are mechanically *identical* with the vapor molecules, which clarifies the structure of the solution and reduces the necessary amount of computation dramatically. The same analysis was applied recently to the case where the vapor is condensing onto the condensed phase at incidence in Ref. 2, where the necessity of considering such a case is explained. In this reference, we restricted ourselves to the case where the magnitude of the flow-velocity component perpendicular to the condensed phase at infinity is less than the sonic speed there (subsonic condensation). In the present paper, we investigate the same problem in the case where it is equal to or greater than the sonic speed (supersonic condensation). Again, the analysis is a straightforward extension of that of Refs. 1 and 3 to the case of condensation at incidence.

[a]Electronic mail: aoki@aero.mbox.media.kyoto-u.ac.jp

The importance of the present problem comes from the following fact: the parameter relation mentioned in the first paragraph in the present section provides the boundary condition for the Euler set of equations on the condensing surface when a steady flow of a vapor around its condensed phases is considered in the continuum limit (the limit where the mean free path of the vapor molecules vanishes) in the presence of a trace of a noncondensable gas. The reader is referred to Ref. 4 for the details. Since the numerically constructed parameter relation plays the role of the numerical boundary condition for the Euler set of equations (see Ref. 4 for its application to a practical problem), we need to present a large amount of numerical data. This is the reason why we split the paper into two parts. In addition, as in Ref. 2, we will make use of the Electronic Physics Auxiliary Publication Service (EPAPS) to reduce the amount of the data contained in the paper.

II. PROBLEM AND ASSUMPTION

A. Problem

To begin with, we repeat the problem that is described in Ref. 2. Consider a vapor in a half space $X_1>0$ bounded by a stationary plane condensed phase of the vapor located at $X_1=0$, where X_i is a rectangular coordinate system. There is a uniform vapor flow at infinity toward the condensed phase with velocity $(v_{\infty 1},v_{\infty 2},0)$ $(v_{\infty 1}<0,\ v_{\infty 2}\geqslant 0)$, temperature T_∞, and pressure p_∞. The condensed phase is kept at a constant and uniform temperature T_w. Steady condensation of the vapor is taking place on the condensed phase, and another gas neither condensing nor evaporating on the condensed phase, which we call the noncondensable gas, is confined near the condensed phase by the condensing vapor flow. (See Fig. 1.) We investigate the steady behavior of the vapor and the noncondensable gas on the basis of kinetic theory.

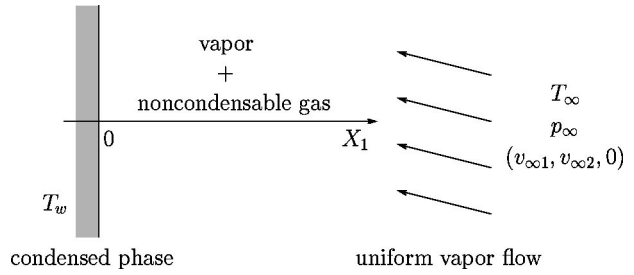

FIG. 1. Uniform flow of a vapor condensing onto its plane condensed phase at incidence in the presence of a noncondensable gas.

Our basic assumptions are as follows: (i) the behavior of the vapor and the noncondensable gas is described by the Boltzmann equation for a binary mixture [the Garzó–Santos–Brey (GSB) model[5] will be employed for numerical computation]; (ii) the vapor molecules leaving the condensed phase are distributed according to the corresponding part of the Maxwellian distribution describing the saturated equilibrium state at rest at temperature T_w; (iii) the noncondensable-gas molecules leaving the condensed phase are distributed according to the corresponding part of the Maxwellian distribution with temperature T_w and flow velocity 0, and there is no net particle flow across the condensed phase (diffuse reflection); (iv) the molecules of the noncondensable gas are mechanically identical with those of the vapor.

B. Relevant parameters

As in Ref. 2, we assign label A to the vapor (it will also be called A-component) and label B to the noncondensable gas (it will also be called B-component) throughout the paper.

The explicit form of the basic equation and boundary condition for the present problem as well as the definition of the macroscopic quantities is given in Ref. 2. To be more specific, the basic equation and its boundary condition are given by Eqs. (2)–(5b) in Ref. 2, and the macroscopic quantities are defined by Eqs. (10a)–(10f) there. Therefore, we omit them here for conciseness.

Now, let p_w be the saturation pressure of the vapor at temperature T_w, and let $M_{n\infty}$ and $M_{t\infty}$ be the normal and tangential Mach numbers of the vapor at infinity, respectively:

$$M_{n\infty}=-\frac{v_{\infty 1}}{\sqrt{5kT_\infty/3m^A}},\quad M_{t\infty}=\frac{v_{\infty 2}}{\sqrt{5kT_\infty/3m^A}}, \tag{1}$$

where k is the Boltzmann constant and m^A is the mass of a molecule of the vapor, which is the same as that of the noncondensable gas because of assumption (iv). According to Ref. 2, the present (dimensionless) boundary-value problem is characterized by the following set of parameters:

$$M_{n\infty},\quad M_{t\infty},\quad T_\infty/T_w,\quad p_\infty/p_w,\quad \Gamma, \tag{2}$$

where Γ is the dimensionless parameter corresponding to the amount of the noncondensable gas contained in the system and defined as follows:

$$\Gamma=\frac{2}{\sqrt{\pi}}\frac{1}{n_\infty l_\infty}\int_0^\infty n^B\,dX_1, \tag{3}$$

where $n_\infty=p_\infty/kT_\infty$ is the molecular number density of the vapor at infinity, n^B the molecular number density of the noncondensable gas, and l_∞ the mean free path of the vapor molecules in the equilibrium state at rest with temperature T_∞ and number density n_∞ (or pressure p_∞); e.g., $l_\infty=[\sqrt{2}\pi(d^A)^2n_\infty]^{-1}$ for the hard-sphere molecules, where d^A is the diameter of a vapor molecule, and $l_\infty=(2/\sqrt{\pi})\times(2kT_\infty/m^A)^{1/2}/K^{AA}n_\infty$ for the GSB model, where K^{AA} is a constant (see Appendix B of Ref. 2). The aim of the present study is to investigate the relation to be satisfied by the five parameters in Eq. (2) in the case of supersonic condensation.

III. MECHANICALLY IDENTICAL MOLECULES

As described in Ref. 2, the assumption (iv) in Sec. II A that the molecules of the noncondensable gas are mechanically identical with those of the vapor simplifies the analysis dramatically. That is, the original problem of two coupled nonlinear equations is decomposed into two single boundary-value problems: a nonlinear problem for the total mixture and a linear homogeneous problem for the noncondensable gas. This approach was originally introduced in Ref. 1 for the case of $M_{t\infty}=0$. Since the approach plays an important role in the following analysis, we first summarize its outline (Sec. III A) and then investigate the relation among the parameters in the case $M_{n\infty}\geqslant 1$ that was omitted in Ref. 2 (Sec. III B).

A. Outline of analysis

Let F^A be the velocity distribution function of the vapor and F^B that of the noncondensable gas, and let $(\hat{F}^A,\hat{F}^B)=n_\infty^{-1}(2kT_\infty/m^A)^{3/2}(F^A,F^B)$ be their dimensionless counterparts. The original problem is a boundary-value problem of the simultaneous nonlinear Boltzmann equations for $(\hat{F}^A,\hat{F}^B)$. We now introduce the (dimensionless) velocity distribution function of the total mixture $\hat{F}=\hat{F}^A+\hat{F}^B$ and transform the boundary-value problem for $(\hat{F}^A,\hat{F}^B)$ to the problem for $(\hat{F},\hat{F}^B)$. The result of the transformation is given by Eqs. (14a)–(17b) in Ref. 2. This transformation essentially decomposes the problem into two separate problems, one for $\hat{F}$ and the other for $\hat{F}^B$, as described below.

The equation for $\hat{F}$ [Eq. (14a) in Ref. 2] is the Boltzmann equation for a single-component gas, and the boundary condition for $\hat{F}$ [Eq. (15a) in Ref. 2] contains a quantity denoted by n_0 that depends on $\hat{F}^B$. However, if we regard this n_0 as the saturation number density of the vapor at temperature T_w, or equivalently, $p_0=kn_0T_w$ as the corresponding saturation pressure, then the equation and boundary condition mentioned above reduce to a closed problem for $\hat{F}$, i.e., the half-space problem of condensation of a pure vapor ($\hat{F}$ plays the role of the velocity distribution function of the pure vapor), which has been investigated by many authors (e.g., Refs. 6–17). The problem is characterized by the following four parameters:

$$M_{n\infty}, \quad M_{t\infty}, \quad T_\infty/T_w, \quad p_\infty/p_0, \tag{4}$$

where we have used p_0 rather than n_0. According to Refs. 6–9 and 12–14, there is a solution only when these parameters satisfy a certain relation, which is expressed as follows:

$$\frac{p_\infty}{p_0} = F_s\left(M_{n\infty}, M_{t\infty}, \frac{T_\infty}{T_w}\right) \quad (M_{n\infty}<1), \tag{5a}$$

$$\frac{p_\infty}{p_0} \geqslant F_b\left(1, M_{t\infty}, \frac{T_\infty}{T_w}\right) \quad (M_{n\infty}=1), \tag{5b}$$

$$\frac{p_\infty}{p_0} > F_b\left(M_{n\infty}, M_{t\infty}, \frac{T_\infty}{T_w}\right) \quad (M_{n\infty}>1). \tag{5c}$$

Comprehensive numerical data for the functions F_s and F_b based on the Bhatnagar–Gross–Krook (BGK) model[18,19] are obtained in Ref. 9. These data show the following properties of the functions F_s and F_b: (i) both functions are weakly dependent on $M_{t\infty}$ and T_∞/T_w; (ii) for any fixed $M_{t\infty}$ and T_∞/T_w, F_s is a monotonically increasing function of $M_{n\infty}$, whereas F_b is a monotonically decreasing function of $M_{n\infty}$; (iii) $F_s(0,0,1)=F_s(0_+,M_{t\infty},T_\infty/T_w)=1$ and $F_s(1_-,M_{t\infty},T_\infty/T_w)=F_b(1,M_{t\infty},T_\infty/T_w)$ (see, e.g., Ref. 13). Thus, in order to have a solution $\hat{F}$, one needs to specify three parameters out of the four parameters in Eq. (4) when $M_{n\infty}<1$ (subsonic condensation), and all the four parameters satisfying the inequality (5b) or (5c) when $M_{n\infty}\geqslant 1$ (supersonic condensation).

Suppose that we have obtained the solution $\hat{F}$ for a given value of n_0. Then, the boundary-value problem for $\hat{F}^B$ [Eqs. (14b), (15b), (16b), and (17b) in Ref. 2] reduces to a linear homogeneous boundary-value problem. Thus, a solution $\hat{F}^B$ multiplied by an arbitrary constant is also a solution. The unique solution is determined by specifying the total amount of the noncondensable gas or, equivalently, the parameter Γ [Eq. (3)]. As in Ref. 2, we denote by $\hat{F}^B_*$ the solution when σ^B_w in Eq. (15b) of Ref. 2 is equal to n_0 (this corresponds to the case of $p_w=0$, i.e., the case where no vapor molecules are emitted from the condensed phase) and by Γ_* the corresponding Γ. Then the solution $\hat{F}^B$ for an arbitrary Γ is expressed as [Eq. (20) in Ref. 2]

$$\hat{F}^B = (\Gamma/\Gamma_*)\hat{F}^B_*, \tag{6}$$

and, therefore, the corresponding $\hat{F}^A$ is given by

$$\hat{F}^A = \hat{F} - (\Gamma/\Gamma_*)\hat{F}^B_*. \tag{7}$$

The $\hat{F}^A$ and $\hat{F}^B$ thus obtained solve the original boundary-value problem with the saturation pressure p_w given by

$$p_w = (1-\Gamma/\Gamma_*)p_0, \tag{8}$$

in terms of p_0 (the virtual saturation pressure). Since p_w is non-negative physically, we obtain from Eq. (8) that

$$0 \leqslant \Gamma \leqslant \Gamma_*. \tag{9}$$

From Eqs. (5a)–(5c) and (8) and the structure of the solution, we can derive the fundamental property of the relation among the parameters that we are seeking. In the case of subsonic condensation ($M_{n\infty}<1$) which is considered in Ref. 2 (see Sec. III D of the same reference), the Γ_* turns out to be a function of the three parameters $M_{n\infty}$, $M_{t\infty}$, T_∞/T_w, and the relation among the parameters takes the following form:

$$p_\infty/p_w = \mathcal{F}_s(M_{n\infty}, M_{t\infty}, T_\infty/T_w, \Gamma), \tag{10}$$

where

$$\mathcal{F}_s(M_{n\infty}, M_{t\infty}, T_\infty/T_w, \Gamma) = \left(1-\frac{\Gamma}{\Gamma_*(M_{n\infty}, M_{t\infty}, T_\infty/T_w)}\right)^{-1} \times F_s(M_{n\infty}, M_{t\infty}, T_\infty/T_w). \tag{11}$$

Comprehensive numerical data, based on the BGK model, for the function F_s are available in Ref. 9 (see also Ref. 2), while those for the function Γ_* are constructed in Ref. 2 using the GSB model that is compatible with the BGK model. Therefore, we now have the numerical data for the function $\mathcal{F}_s$. It should be noted that the dependence of $\mathcal{F}_s$ on Γ is explicit.

B. Existence range of a solution: Supersonic condensation

Next, we investigate the relation among the parameters $M_{n\infty}$, $M_{t\infty}$, T_∞/T_w, p_∞/p_w, and Γ that allows a solution in the case of supersonic condensation ($M_{n\infty}\geqslant 1$). The description below is essentially the same as that in Ref. 1. For the problem of $\hat{F}$, we can freely choose the parameters $M_{n\infty}$, $M_{t\infty}$, T_∞/T_w, and p_∞/p_0 satisfying the relation (5b) or (5c), and hence the solution $\hat{F}$ depends on these four parameters. On the other hand, the problem for $\hat{F}^B_*$ contains the parameters $M_{n\infty}$, $M_{t\infty}$, T_∞/T_w, and p_∞/p_0 through $\hat{F}$. Therefore, $\hat{F}^B_*$ and thus Γ_*, which is obtained from $\hat{F}^B_*$, are the functions of $M_{n\infty}$, $M_{t\infty}$, T_∞/T_w, and p_∞/p_0. Thus we may write Eq. (8) explicitly as

$$p_\infty/p_w = \left(1-\frac{\Gamma}{\Gamma_*(M_{n\infty}, M_{t\infty}, T_\infty/T_w, p_\infty/p_0)}\right)^{-1} \times p_\infty/p_0, \tag{12}$$

and Eq. (9) as

$$0 \leqslant \Gamma \leqslant \Gamma_*(M_{n\infty}, M_{t\infty}, T_\infty/T_w, p_\infty/p_0). \tag{13}$$

Now, let us suppose that Γ_* is a decreasing function of p_∞/p_0. (It is numerically confirmed in Ref. 1 that Γ_* is a monotonically decreasing function of p_∞/p_0 when $M_{t\infty}=0$.) This hypothesis will be confirmed numerically in Sec. IV A below. Then, for fixed $M_{n\infty}$, $M_{t\infty}$, T_∞/T_w, and Γ, the range of p_∞/p_0 is from F_b [Eq. (5c)] to the value of p_∞/p_0 such that $\Gamma_*(M_{n\infty}, M_{t\infty}, T_\infty/T_w, p_\infty/p_0)=\Gamma$ holds, since Γ_* cannot be less than Γ by Eq. (13). When p_∞/p_0 ranges in this interval, p_∞/p_w ranges from $[1-\Gamma/\Gamma_*(M_{n\infty}, M_{t\infty}, T_\infty/T_w, p_\infty/p_0 \to F_b)]^{-1}F_b$ to infinity because the right-hand side of Eq. (12) is an increasing function of p_∞/p_0.

To summarize, in the case of supersonic condensation, there exists a solution only when the parameters satisfy the following relation:

$$\frac{p_\infty}{p_w} > \mathcal{F}_b(M_{n\infty}, M_{t\infty}, T_\infty/T_w, \Gamma), \quad (M_{n\infty} > 1), \tag{14a}$$

$$\frac{p_\infty}{p_w} \geqslant \mathcal{F}_b(1, M_{t\infty}, T_\infty/T_w, \Gamma), \quad (M_{n\infty} = 1), \tag{14b}$$

where

$$\mathcal{F}_b(M_{n\infty}, M_{t\infty}, T_\infty/T_w, \Gamma) = \left(1 - \frac{\Gamma}{\Gamma_b(M_{n\infty}, M_{t\infty}, T_\infty/T_w)}\right)^{-1} \times F_b(M_{n\infty}, M_{t\infty}, T_\infty/T_w), \tag{15a}$$

$$\Gamma_b(M_{n\infty}, M_{t\infty}, T_\infty/T_w) = \Gamma_*(M_{n\infty}, M_{t\infty}, T_\infty/T_w, p_\infty/p_0 \to F_b). \tag{15b}$$

As in the case of subsonic condensation,[2] if we exploit the comprehensive numerical data for F_b based on the BGK model given in Ref. 9, we just need to compute Γ_b for various values of the set $(M_{n\infty}, M_{t\infty}, T_\infty/T_w)$, making use of a model Boltzmann equation compatible with the BGK model. In this way, we can construct the function $\mathcal{F}_b$. It should be stressed that, since the Γ-dependence of $\mathcal{F}_b$ is explicit, we are able to construct $\mathcal{F}_b$ of four variables by obtaining the function Γ_b of three variables. This reduces the amount of necessary computation dramatically. We will carry out the actual numerical computation to obtain Γ_b in the next section.

IV. NUMERICAL ANALYSIS AND RESULTS

In this section, we carry out actual numerical analysis to obtain Γ_b. As in Refs. 1–3, we employ the GSB model[5] of the Boltzmann equation, which is summarized in Appendix B of Ref. 2. We solve the problem by means of a finite-difference method. Since the solution method is essentially the same as that given in Ref. 9 for the case of a single-component system, we omit it here. See also Sec. IV A of Ref. 2 for some remarks on numerical analysis. Information about the accuracy of the present computation is given in the Appendix.

A. Existence range of a solution

In this section, we show some numerical results for the existence range of a solution discussed in Sec. III B. First, we confirm the assumption we made in Sec. III B, namely, $\Gamma_*(M_{n\infty}, M_{t\infty}, T_\infty/T_w, p_\infty/p_0)$ is a decreasing function in p_∞/p_0 (this has already been confirmed numerically in Ref. 1 for the case $M_{t\infty}=0$). The Γ_* versus p_∞/p_0 for various values of $M_{n\infty}$ and $M_{t\infty}$ in the case of $T_\infty/T_w=1$ are shown in Fig. 2. Clearly, the function Γ_* is decreasing in p_∞/p_0. It is true also for other values of T_∞/T_w. Hence the discussion in Sec. III B is valid, and the existence range of a solution is given by Eqs. (14a)–(15b).

Once we have the data for the functions F_b and Γ_b, Eq. (15a) gives the function $\mathcal{F}_b$ immediately. In principle, F_b can be constructed by trying to obtain the solution $\hat{F}$ for many sets of values of the parameters $(M_{n\infty}, M_{t\infty}, T_\infty/T_w, p_\infty/p_0)$. However, since such an approach is not practical, another indirect method was used in Ref. 9 to obtain numerical values of F_b, which will be explained below. Now let us suppose that F_b is known and recall that Γ_b is the limiting value of $\Gamma_*(M_{n\infty}, M_{t\infty}, T_\infty/T_w, p_\infty/p_0)$ as $p_\infty/p_0 \to F_b(M_{n\infty}, M_{t\infty}, T_\infty/T_w)$ [see Eq. (15b)]. The straightfor-

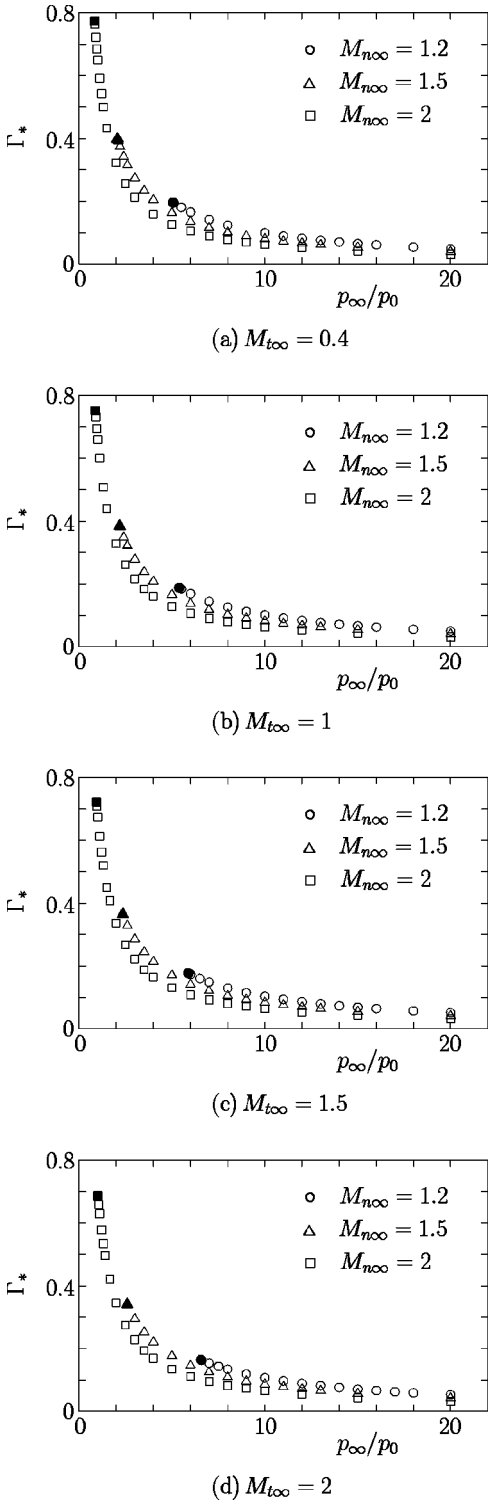

FIG. 2. $\Gamma_*(M_{n\infty}, M_{t\infty}, T_\infty/T_w, p_\infty/p_0)$ vs p_∞/p_0 for various $M_{n\infty}$ and $M_{t\infty}$ in the case of $T_\infty/T_w=1$. (a) $M_{t\infty}=0.4$, (b) $M_{t\infty}=1$, (c) $M_{t\infty}=1.5$, and (d) $M_{t\infty}=2$. The symbols in black represent the limiting values of $\Gamma_*(M_{n\infty}, M_{t\infty}, T_\infty/T_w, p_\infty/p_0)$ as $p_\infty/p_0 \to F_b$.

ward way to compute this limit is to obtain the solution ($\hat{F}$, $\hat{F}^B_*$) for several values of p_∞/p_0 close enough to F_b and deduce the limit of Γ_* by extrapolation. However, as p_∞/p_0 approaches F_b, the computation for obtaining $\hat{F}$ becomes increasingly difficult (note that there is no solution at $p_\infty/p_0=F_b$). Therefore, such a method is not practical. This situation is the same as that in Ref. 1 for the case $M_{t\infty}=0$, where a different (indirect) method to obtain Γ_b is proposed. We make use of the same method, which will be described, together with the method for obtaining F_b, in the following.

According to Refs. 7–9, the behavior of $\hat{F}$ for ($M_{n\infty}$, $M_{t\infty}$, T_∞/T_w, p_∞/p_0) with p_∞/p_0 close to $F_b(M_{n\infty},M_{t\infty},T_\infty/T_w)$ is summarized as follows.

(i) When p_∞/p_0 is sufficiently close to $F_b(M_{n\infty},M_{t\infty},T_\infty/T_w)$, the solution $\hat{F}$ is described as follows: the part near the condensed phase is almost a subsonic solution (a solution with $M_{n\infty}<1$), and this part is followed by an almost entire profile of a standing shock, parallel to the condensed phase, whose upstream state is the state at infinity (p_∞, T_∞, $M_{n\infty}$, $M_{t\infty}$). As p_∞/p_0 approaches F_b, the position of the standing shock moves upstream, and the separation between the subsonic-solution part and the standing-shock part becomes clearer.

(ii) In the limit $p_\infty/p_0\to F_b$, the position of the standing shock moves to upstream infinity, and thus the separation becomes complete. This means that the limiting solution is a subsonic solution with a standing shock at infinity and thus is not a true supersonic solution. However, we can interpret it as the marginal supersonic solution. Therefore the limiting solution is the subsonic solution with the upstream parameters $M'_{n\infty}$, $M'_{t\infty}$, and T'_∞ [thus $p'_\infty=p_0F_s(M'_{n\infty},M'_{t\infty},T'_\infty/T_w)$], where $M'_{n\infty}$, $M'_{t\infty}$, and T'_∞ are given by the standing shock relation (Rankine–Hugoniot relation) from $M_{n\infty}$, $M_{t\infty}$, and T_∞ as follows:

$$M'_{n\infty}=(M^2_{n\infty}+3)^{1/2}(5M^2_{n\infty}-1)^{-1/2}, \tag{16a}$$

$$M'_{t\infty}=\left(\frac{T_\infty}{T_w}\right)^{1/2}\left(\frac{T'_\infty}{T_w}\right)^{-1/2}M_{t\infty}, \tag{16b}$$

$$\frac{T'_\infty}{T_w}=\frac{(M^2_{n\infty}+3)(5M^2_{n\infty}-1)}{16M^2_{n\infty}}\frac{T_\infty}{T_w}. \tag{16c}$$

Equation (16b) indicates the continuity of the tangential velocity component across the shock. Since the shock relation also gives

$$\frac{p'_\infty}{p_0}=\frac{5M^2_{n\infty}-1}{4}\frac{p_\infty}{p_0}, \tag{17}$$

the F_b, which corresponds to p_∞/p_0, is obtained as

$$F_b(M_{n\infty},M_{t\infty},T_\infty/T_w)=\frac{4}{5M^2_{n\infty}-1}F_s(M'_{n\infty},M'_{t\infty},T'_\infty/T_w). \tag{18}$$

The behavior described above is based on physical consideration with some numerical evidence.[9] For $M_{n\infty}$ close to unity, however, it has been justified analytically in Ref. 12. Although $M_{t\infty}=0$ is assumed in this reference, it is not essential for the analysis there.

Since $\hat{F}^B_*$ vanishes at infinity in the subsonic solution, the limiting value of $\int_0^\infty n^B dX_1$ as $p_\infty/p_0\to F_b$ is equal to the value calculated from the corresponding subsonic solution, i.e., the solution with the parameters $M'_{n\infty}$, $M'_{t\infty}$, and T'_∞ (thus p'_∞) at infinity. Taking account of this fact, we obtain from Eq. (3) that $n_\infty l_\infty\Gamma_b=n'_\infty l'_\infty\Gamma_*$, where $n'_\infty=p'_\infty/kT'_\infty$ and l'_∞ is the mean free path of the vapor in the equilibrium state at rest with temperature T'_∞ and number density n'_∞. Since $n'_\infty l'_\infty/n_\infty l_\infty=(T'_\infty/T_\infty)^{1/2}$ holds for the GSB model (see the last paragraph of Sec. II B), we obtain the formula

$$\Gamma_b(M_{n\infty},M_{t\infty},T_\infty/T_w)=\left(\frac{T'_\infty}{T_w}\right)^{1/2}\left(\frac{T_\infty}{T_w}\right)^{-1/2}\Gamma_*(M'_{n\infty},M'_{t\infty},T'_\infty/T_w). \tag{19}$$

From Eqs. (16a)–(16c) and (18), we can obtain F_b immediately for any $M_{n\infty}$, $M_{t\infty}$, and T_∞/T_w by using the numerical data of F_s tabulated in Ref. 9 (see also Ref. 2) and interpolation. In Ref. 9, however, for the purpose of presenting accurate numerical values of F_b in a well-arranged way, the subsonic solution $\hat{F}$ for each set of ($M'_{n\infty}$, $M'_{t\infty}$, T'_∞/T_w) ($M'_{n\infty}<1$) given by Eqs. (16a)–(16c) was recomputed to obtain F_s, from which F_b was obtained by Eq. (18) without the help of interpolation. More specifically, Fig. 7 and Tables V–VIII in Ref. 9 show the numerical data of $F_b(M_{n\infty},M_{t\infty},T_\infty/T_w)$ for $T_\infty/T_w=0.5$, 1, 1.5, and 2 obtained in this way. In the present study, we have repeated the same computation with higher accuracy and confirmed the accuracy of the data given in Ref. 9. The results are as follows: in Tables VI–VIII in Ref. 9, the last figure should be changed by one in several data, and in Table V there, the last figure should be changed by one in five data for $M_{n\infty}=1.2$ and by at most six in the data for $M_{n\infty}=1.1$ and 1.01. We also made additional computations to supplement these data. Some of the results are shown in Table I, the more comprehensive data being given in Tables I–IV in Ref. 20.

Similarly, from Eqs. (16a)–(16c) and (19), we can obtain Γ_b using the numerical values of Γ_* for subsonic solutions tabulated in Ref. 2 with the help of interpolation. But, in order to give accurate numerical data in a well-arranged way, we recompute $\hat{F}^B_*$ that corresponds to the subsonic solution $\hat{F}$ obtained above [i.e., the subsonic solution for $(M'_{n\infty},M'_{t\infty},T'_\infty/T_w)$ given by Eqs. (16a)–(16c)] and obtain Γ_* for this $\hat{F}^B_*$. Thus, we obtain accurate numerical values of Γ_b by Eq. (19) without using interpolation. Some of the results for Γ_b obtained in this way are shown in Table II, the more comprehensive data being given in Tables V–VIII in Ref. 20.

The function $\mathcal{F}_b$ obtained with the help of the numerical data for F_b and Γ_b in the case $T_\infty/T_w=1$ is shown in Fig. 3. In the figure, $\mathcal{F}_b$ versus $M_{n\infty}$ is shown for various Γ at four values of $M_{t\infty}$, i.e., $M_{t\infty}=0$, 1, 2, and 3. Similar figures for $T_\infty/T_w=0.5$, 1.5, and 2 are given in Figs. 1, 3, and 4 in Ref. 20 (Fig. 2 in Ref. 20 is the same as Fig. 3 here). The $\mathcal{F}_b$ is a decreasing function of $M_{n\infty}$, and its curve moves upward as

TABLE I. $F_b(M_{n\infty}, M_{t\infty}, T_\infty/T_w)$ as a function of $M_{n\infty}$, $M_{t\infty}$, and T_∞/T_w.

	$T_\infty/T_w=0.5$				$T_\infty/T_w=1$			
$M_{n\infty}\backslash M_{t\infty}$	0	1	2	3	0	1	2	3
1	17.304	18.292	21.258	26.205	13.549	14.680	18.074	23.734
1.005	16.652	17.604	20.460	25.223	13.118	14.212	17.494	22.970
1.01	16.025	16.941	19.691	24.278	12.702	13.760	16.935	22.232
1.05	12.117	12.811	14.893	18.364	10.000	10.825	13.300	17.429
1.1	9.0094	9.5220	11.060	13.626	7.7043	8.3293	10.205	13.334
1.2	5.5876	5.8975	6.8275	8.3784	5.0021	5.3916	6.5608	8.5108
1.3	3.8254	4.0304	4.6455	5.6712	3.5256	3.7876	4.5743	5.8863
1.4	2.7941	2.9381	3.3702	4.0907	2.6289	2.8149	3.3735	4.3050
1.5	2.1369	2.2426	2.5597	3.0884	2.0426	2.1801	2.5929	3.2814
1.6	1.6917	1.7719	2.0125	2.4136	1.6378	1.7426	2.0574	2.5823
1.7	1.3757	1.4382	1.6256	1.9381	1.3461	1.4281	1.6742	2.0845
1.8	1.1431	1.1928	1.3419	1.5906	1.1288	1.1942	1.3906	1.7180
2.0	0.829 58	0.862 70	0.962 08	1.1278	0.831 83	0.875 60	1.0069	1.2259
2.5	0.451 22	0.465 90	0.509 96	0.583 39	0.465 24	0.484 74	0.543 23	0.640 71
3.0	0.289 23	0.297 02	0.320 41	0.359 39	0.304 28	0.314 65	0.345 77	0.397 60
	$T_\infty/T_w=1.5$				$T_\infty/T_w=2$			
$M_{n\infty}\backslash M_{t\infty}$	0	1	2	3	0	1	2	3
1	12.401	13.651	17.270	23.666	11.916	13.270	17.337	24.123
1.005	12.038	13.249	16.886	22.954	11.584	12.898	16.843	23.426
1.01	11.686	12.861	16.386	22.266	11.263	12.537	16.365	22.752
1.05	9.3645	10.291	13.074	17.715	9.1182	10.132	13.175	18.252
1.1	7.3326	8.0428	10.175	13.731	7.2088	7.9903	10.337	14.252
1.2	4.8647	5.3134	6.6605	8.9076	4.8453	5.3431	6.8378	9.3314
1.3	3.4771	3.7814	4.6950	6.2188	3.4929	3.8320	4.8505	6.5495
1.4	2.6188	2.8360	3.4878	4.5751	2.6468	2.8895	3.6184	4.8342
1.5	2.0505	2.2115	2.6948	3.5011	2.0820	2.2624	2.8039	3.7072
1.6	1.6542	1.7773	2.1467	2.7628	1.6860	1.8240	2.2384	2.9297
1.7	1.3666	1.4630	1.7523	2.2347	1.3972	1.5054	1.8303	2.3720
1.8	1.1510	1.2281	1.4592	1.8446	1.1799	1.2665	1.5262	1.9593
2.0	0.854 41	0.906 01	1.0609	1.3190	0.879 70	0.937 74	1.111 92	1.4023
2.5	0.484 24	0.507 28	0.576 38	0.691 54	0.502 59	0.528 53	0.606 34	0.736 03
3.0	0.319 75	0.332 01	0.368 80	0.430 09	0.333 80	0.347 62	0.389 06	0.458 10

Γ increases. The Γ_c in the figures, which depends on $M_{t\infty}$ and T_∞/T_w, is a critical value of Γ, that is, when $\Gamma<\Gamma_c$, $\mathcal{F}_b$ takes a finite value at $M_{n\infty}=1$, whereas when $\Gamma>\Gamma_c$, $\mathcal{F}_b$ becomes infinitely large as $M_{n\infty}$ approaches a certain value of $M_{n\infty}$ depending on $M_{t\infty}$, T_∞/T_w, and Γ. We denote this value by $\tilde{M}_c$. When $\Gamma=\Gamma_c$, $\mathcal{F}_b$ goes to infinity at $M_{n\infty}=1$ (hence $\tilde{M}_c=1$). In other words, $M_{n\infty}=\tilde{M}_c$ is the asymptote of the curve. Consequently, there is no solution in the interval $1\leqslant M_{n\infty}\leqslant\tilde{M}_c$ when $\Gamma>\Gamma_c$. Further properties of $\mathcal{F}_b$ will be discussed in the next paragraph, where more detailed information about Γ_c and $\tilde{M}_c$ will also be given.

Because the dependence of F_b and Γ_b on $M_{t\infty}$ is not strong, the function $\mathcal{F}_b$ does not depend much on $M_{t\infty}$. Therefore the features of $\mathcal{F}_b$ are essentially the same as those described in Refs. 1 and 3 for $M_{t\infty}=0$. In particular, for $M_{t\infty}$ smaller than around 1, $\mathcal{F}_b$ is almost independent of $M_{t\infty}$. The dependence of $\mathcal{F}_b$ on T_∞/T_w is also weak (see Figs. 1–4 in Ref. 20). The F_b is a decreasing function of $M_{n\infty}$, whereas Γ_b is its increasing function. Therefore, as is seen from Eq. (15a), $\mathcal{F}_b$ is a decreasing function of $M_{n\infty}$. It follows from Eqs. (16a)–(16c), (18), and (19) that at $M_{n\infty}=1$, the following relations hold:

$$F_b(1,M_{t\infty},T_\infty/T_w)=F_s(1_-,M_{t\infty},T_\infty/T_w), \tag{20a}$$

$$\Gamma_b(1,M_{t\infty},T_\infty/T_w)=\Gamma_*(1_-,M_{t\infty},T_\infty/T_w)\equiv\Gamma_c(M_{t\infty},T_\infty/T_w), \tag{20b}$$

where Γ_c is the same as that used in Ref. 2. Analytical evidence for the relation (20a) is found in Ref. 12. Then, the properties of $\mathcal{F}_b$ described in the preceding paragraph follow immediately from Eqs. (15a) and (20b) and from the fact that Γ_b is an increasing function of $M_{n\infty}$. That is, when $\Gamma<\Gamma_c$, the Γ/Γ_b in Eq. (15a) is less than unity and thus $\mathcal{F}_b$ remains finite in the whole range of $M_{n\infty}\geqslant 1$. From Eqs. (11), (15a), (20a), and (20b), we have

$$\mathcal{F}_b(1,M_{t\infty},T_\infty/T_w,\Gamma)=\mathcal{F}_s(1_-,M_{t\infty},T_\infty/T_w,\Gamma), \tag{21}$$

in this case. When $\Gamma>\Gamma_c$ (or $\Gamma=\Gamma_c$), the Γ/Γ_b in Eq. (15a) becomes unity at an $M_{n\infty}(>1)$ (or at $M_{n\infty}=1$). If we denote this value of $M_{n\infty}$ by $\tilde{M}_c$ ($\tilde{M}_c=1$ for $\Gamma=\Gamma_c$), $\mathcal{F}_b$ increases indefinitely as $M_{n\infty}$ approaches $\tilde{M}_c$. The Γ_c, which is a function of $M_{t\infty}$ and T_∞/T_w, is shown in Fig. 3 of Ref. 2. The $\tilde{M}_c(M_{t\infty},T_\infty/T_w,\Gamma)$, which is the solution of

TABLE II. $\Gamma_b(M_{n\infty}, M_{t\infty}, T_\infty/T_w)$ as a function of $M_{n\infty}$, $M_{t\infty}$, and T_∞/T_w.

	$T_\infty/T_w=0.5$				$T_\infty/T_w=1$			
$M_{n\infty}\backslash M_{t\infty}$	0	1	2	3	0	1	2	3
1	0.059 725	0.057 473	0.051 952	0.045 488	0.085 603	0.080 878	0.070 154	0.058 957
1.005	0.061 829	0.059 494	0.053 770	0.047 069	0.088 071	0.083 214	0.072 187	0.060 667
1.01	0.063 971	0.061 552	0.055 621	0.048 679	0.090 569	0.085 580	0.074 246	0.062 399
1.05	0.081 764	0.078 654	0.071 025	0.062 088	0.111 25	0.105 19	0.091 356	0.076 818
1.1	0.105 56	0.101 55	0.091 706	0.080 132	0.138 72	0.131 29	0.114 24	0.096 179
1.2	0.157 68	0.151 82	0.137 31	0.120 10	0.198 19	0.188 03	0.164 42	0.138 91
1.3	0.214 75	0.207 02	0.187 73	0.164 56	0.262 48	0.249 68	0.219 52	0.186 28
1.4	0.275 70	0.266 13	0.242 10	0.212 83	0.330 42	0.315 13	0.278 64	0.237 61
1.5	0.339 72	0.328 41	0.299 75	0.264 40	0.401 13	0.383 55	0.341 07	0.292 35
1.6	0.406 18	0.393 23	0.360 15	0.318 82	0.473 94	0.454 29	0.406 21	0.350 06
1.7	0.474 60	0.460 13	0.422 87	0.375 75	0.548 37	0.526 85	0.473 62	0.410 37
1.8	0.544 60	0.528 73	0.487 58	0.434 90	0.624 02	0.600 84	0.542 92	0.472 95
2.0	0.688 23	0.669 93	0.621 84	0.558 89	0.777 88	0.751 97	0.685 99	0.603 87
2.5	1.0602	1.0377	0.976 93	0.893 67	1.1699	1.1398	1.0604	0.955 46
3.0	1.4408	1.4161	1.3480	1.2515	1.5642	1.5324	1.4465	1.3280
	$T_\infty/T_w=1.5$				$T_\infty/T_w=2$			
$M_{n\infty}\backslash M_{t\infty}$	0	1	2	3	0	1	2	3
1	0.101 41	0.094 710	0.080 190	0.065 962	0.112 40	0.104 12	0.086 727	0.070 380
1.005	0.104 05	0.097 195	0.082 315	0.067 721	0.115 15	0.106 69	0.088 906	0.072 166
1.01	0.106 72	0.099 705	0.084 464	0.069 500	0.117 93	0.109 29	0.091 105	0.073 969
1.05	0.128 80	0.120 48	0.102 31	0.084 304	0.140 85	0.130 77	0.109 36	0.088 978
1.1	0.158 02	0.148 07	0.126 14	0.104 17	0.171 12	0.159 23	0.133 74	0.109 11
1.2	0.220 95	0.207 79	0.178 28	0.147 97	0.236 09	0.220 70	0.186 99	0.153 48
1.3	0.288 56	0.272 36	0.235 41	0.196 49	0.305 64	0.286 97	0.245 27	0.202 63
1.4	0.359 65	0.340 65	0.296 58	0.249 05	0.378 53	0.356 89	0.307 61	0.255 86
1.5	0.433 30	0.411 77	0.361 06	0.305 09	0.453 66	0.429 56	0.373 26	0.312 62
1.6	0.508 87	0.485 08	0.428 25	0.364 16	0.530 99	0.504 32	0.441 61	0.372 45
1.7	0.585 84	0.560 06	0.497 66	0.425 87	0.609 38	0.580 67	0.512 16	0.434 95
1.8	0.663 84	0.636 33	0.568 91	0.489 89	0.688 68	0.658 21	0.584 52	0.499 77
2.0	0.821 87	0.791 56	0.715 70	0.623 72	0.848 97	0.815 71	0.733 40	0.635 25
2.5	1.2215	1.1873	1.0980	0.982 29	1.2526	1.2157	1.1201	0.997 71
3.0	1.6205	1.5851	1.4900	1.3608	1.6539	1.6161	1.5153	1.3794

$$\Gamma_b(\tilde{M}_c, M_{t\infty}, T_\infty/T_w)=\Gamma, \tag{22}$$

is shown in Fig. 4, where $\tilde{M}_c$ versus $M_{t\infty}$ at $T_\infty/T_w=0.5$, 1, 1.5, and 2 is plotted for various values of Γ; $\tilde{M}_c$ is taken as the abscissa for easy comparison with Fig. 3 (and Figs. 1–4 in Ref. 20).

B. Macroscopic quantities

In this section, we show the behavior of the macroscopic quantities. In the case of supersonic condensation ($M_{n\infty} \geqslant 1$), we can freely choose the parameters ($M_{n\infty}$, $M_{t\infty}$, T_∞/T_w, p_∞/p_w, Γ) in the region (14a) or (14b). However, it is more convenient to arrange the results using the parameters ($M_{n\infty}$, $M_{t\infty}$, T_∞/T_w, p_∞/p_0, Γ) rather than the original parameters ($M_{n\infty}$, $M_{t\infty}$, T_∞/T_w, p_∞/p_w, Γ), since the basic quantities ($\hat{F}$, $\hat{F}^B_*$) and Γ_*, which give the solutions ($\hat{F}^A$, $\hat{F}^B$) for arbitrary Γ, are determined by $M_{n\infty}$, $M_{t\infty}$, T_∞/T_w, and p_∞/p_0. We use the same notations for the macroscopic quantities as in Ref. 2 (cf. Sec. II B of Ref. 2): n^α denotes the molecular number density, v_i^α the flow velocity, T^α the *temperature*, and $p^\alpha(=kn^\alpha T^\alpha)$ the *pressure* of the α component ($\alpha=A$ or B); n denotes the molecular number density, v_i the flow velocity, T the temperature, and p ($=knT$) the pressure of the total mixture. [n^B has already been introduced in Sec. II in the sentence following Eq. (3).]

The typical profiles of the macroscopic quantities for $T_\infty/T_w=1$ are shown in Figs. 5–7, i.e., Fig. 5 for $M_{n\infty}=1.5$ and $p_\infty/p_0=2.593$, Fig. 6 for $M_{n\infty}=2$ and $p_\infty/p_0=4$, and Fig. 7 for $M_{n\infty}=1.05$ and $p_\infty/p_0=22$. In each figure, the result for $M_{t\infty}=1$ is shown in (a) and that for $M_{t\infty}=2$ in (b), and the notation $a_\infty=(5kT_\infty/3m^A)^{1/2}$ has been introduced. It should be noted that $v_1^B\equiv 0$ in the whole region of $X_1>0$, and the quantities $(\Gamma_*/\Gamma)n^B$, v_2^B, $T^B(=p^B/kn^B)$, and $(\Gamma_*/\Gamma)p^B$ are independent of Γ (see Secs. II C and IV C of Ref. 2). The n, v_1, v_2, T, and p for the total mixture are the same as n^A, v_1^A, v_2^A, T^A, and p^A for $\Gamma=0$, respectively.

Figure 5 demonstrates the profiles for the parameters close to the boundary of the existence range (5c) [or Eq. (14a)] (note that $F_b=2.1801$ for $M_{t\infty}=1$ and $F_b=2.5929$ for $M_{t\infty}=2$ in the case $M_{n\infty}=1.5$ and $T_\infty/T_w=1$). Since the parameters for Fig. 5(b) are very close to the boundary of the existence range, the profile exhibits the features described in the fourth paragraph in Sec. IV A, that is, the profile is a combination of a subsonic solution and a standing shock that are well separated from each other. The noncondensable gas

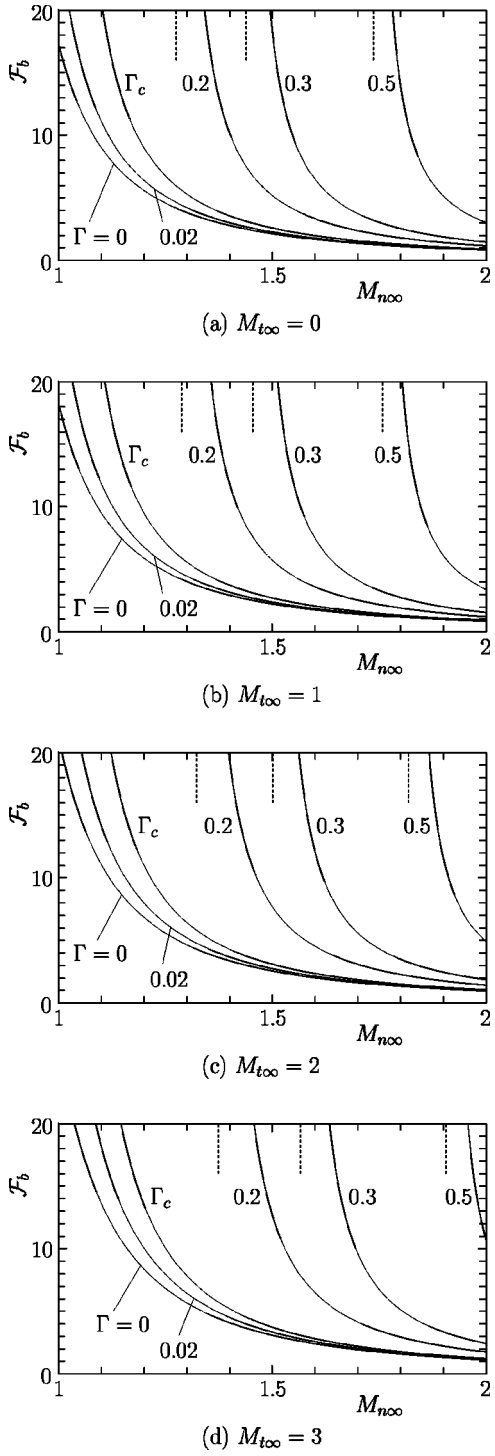

FIG. 3. $\mathcal{F}_b(M_{n\infty}, M_{t\infty}, T_\infty/T_w, \Gamma)$ vs $M_{n\infty}$ for various Γ and $M_{t\infty}$ $(T_\infty/T_w = 1)$. (a) $M_{t\infty}=0$, (b) $M_{t\infty}=1$, (c) $M_{t\infty}=2$, and (d) $M_{t\infty}=3$. The dotted lines in the figures indicate the asymptotes $(M_{n\infty}=\tilde{M}_c)$ of the curves for $\Gamma = 0.2$, 0.3, and 0.5. The value of Γ_c in each figure is as follows: (a) 0.085 603, (b) 0.080 878, (c) 0.070 154, and (d) 0.058 957.

is confined only in the subsonic-solution part. Figure 6 shows the profiles for the parameters well inside the existence range (5c) [or Eq. (14a)] (note that $F_b = 0.875\,60$ for $M_{t\infty}=1$ and $F_b = 1.0069$ for $M_{t\infty}=2$ in the case $M_{n\infty}=2$ and $T_\infty/T_w=1$). These profiles are of the same type as Fig. 11 of Ref. 9. Figure 7, which corresponds to Fig. 12 of Ref.

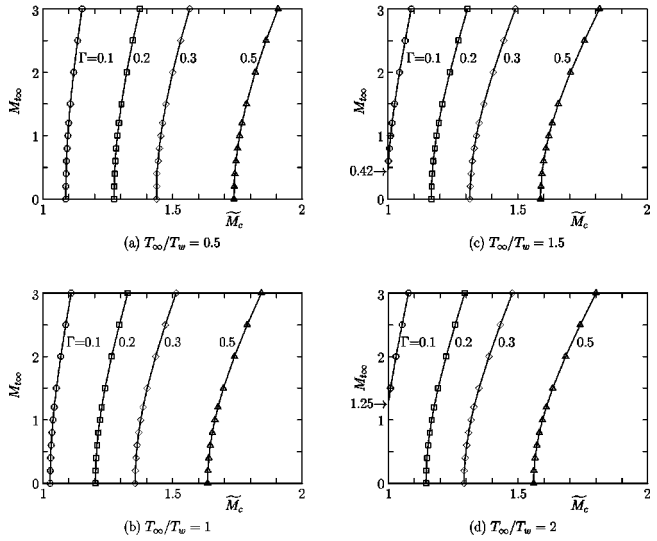

FIG. 4. $\tilde{M}_c$ vs $M_{t\infty}$ for various Γ. (a) $T_\infty/T_w=0.5$, (b) $T_\infty/T_w=1$, (c) $T_\infty/T_w=1.5$, and (d) $T_\infty/T_w=2$. $\tilde{M}_c$ is taken as the abscissa for easy comparison with Fig. 3 (and Figs. 1–4 in Ref. 20). In (c) and (d) the curve for $\Gamma=0.1$ intersects $\tilde{M}_c=1$ at $M_{t\infty}=0.42$ and $M_{t\infty}=1.25$, respectively.

9, shows the profiles for large p_∞/p_0 and $M_{n\infty}$ close to 1 (note that $F_b=10.825$ for $M_{t\infty}=1$ and $F_b=13.300$ for $M_{t\infty}=2$ in the case $M_{n\infty}=1.05$ and $T_\infty/T_w=1$). Since the features of the macroscopic quantities demonstrated in Figs. 5–7 are essentially the same as those already discussed in Ref. 9 for the pure-vapor case $(\Gamma=0)$ and Refs. 1 and 3 in the case of $M_{t\infty}=0$, we omit the repetition of the explanations here.

As discussed in Ref. 1, v_2^B and T^B do not approach $v_{\infty 2}$ and T_∞ and may also have gradients at infinity. In any case, v_2^B and T^B are not meaningful in the far field where n^B becomes practically zero.

C. Particle flux of the noncondensable gas along the condensed phase

As is seen from Figs. 5–7, there is a macroscopic motion of the noncondensable gas along the condensed phase (i.e., in the X_2 direction) when the vapor flow at infinity has a transversal component $(M_{t\infty}\neq 0)$. As in Ref. 2, we introduce the following dimensionless quantity corresponding to the total particle flux of the noncondensable gas:

$$\hat{\mathcal{N}}_f = (2/\sqrt{\pi})[n_\infty l_\infty (2kT_\infty/m^A)^{1/2}]^{-1} \int_0^\infty n^B v_2^B \, dX_1 . \tag{23}$$

Actually, $(\sqrt{\pi}/2) n_\infty l_\infty (2kT_\infty/m^A)^{1/2} \hat{\mathcal{N}}_f$ indicates the total particle flux of the noncondensable gas in the direction of X_2 per unit width in X_3 and per unit time. If we use the definition of the macroscopic quantities and the relation between dimensional and dimensionless quantities given in Ref. 2, Eq. (23) is written in terms of $\hat{F}^B$ as

$$\hat{\mathcal{N}}_f = \int_0^\infty \left(\int \zeta_2 \hat{F}^B d^3\zeta \right) dx_1 , \tag{24}$$

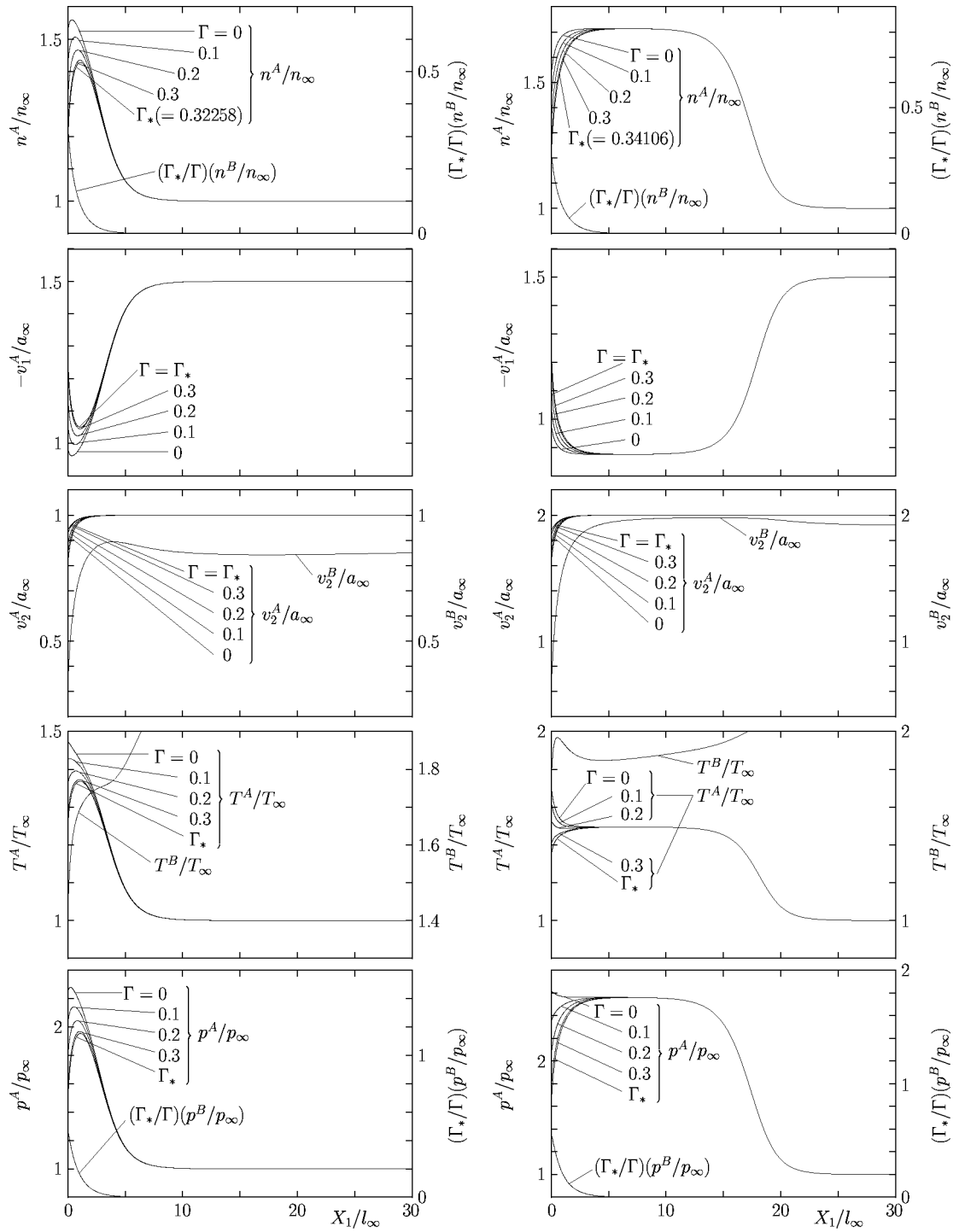

FIG. 5. Profiles of the macroscopic quantities for $M_{n\infty}=1.5$, $T_\infty/T_w=1$, and $p_\infty/p_0=2.593$. (a) $M_{t\infty}=1$ and (b) $M_{t\infty}=2$. Here, $a_\infty=(5kT_\infty/3m^A)^{1/2}$ is the sound speed at temperature T_∞. The macroscopic quantities of the total mixture are given by those of the vapor for $\Gamma=0$. The profiles of $(\Gamma_*/\Gamma)\times(n^B/n_\infty)$, v_2^B/a_∞, T^B/T_∞, and $(\Gamma_*/\Gamma)(p^B/p_\infty)$ are independent of Γ.

where $x_1=(2/\sqrt{\pi})l_\infty^{-1}X_1$ is the dimensionless space coordinate, ζ_i is the dimensionless molecular velocity nondimensionalized by $(2kT_\infty/m^A)^{1/2}$, and $d^3\zeta=d\zeta_1 d\zeta_2 d\zeta_3$; here and in what follows, the domain of integration with respect to ζ_i is the whole space of ζ_i.

Since $\hat{F}^B$ is determined by $M_{n\infty}$, $M_{t\infty}$, T_∞/T_w, p_∞/p_w, and Γ in the case of supersonic condensation, $\hat{\mathcal{N}}_f$ is written in the following form:

$$\hat{\mathcal{N}}_f=\hat{\mathcal{N}}_f\left(M_{n\infty}, M_{t\infty}, \frac{T_\infty}{T_w}, \frac{p_\infty}{p_w}, \Gamma\right), \quad (M_{n\infty}\geqslant 1). \tag{25}$$

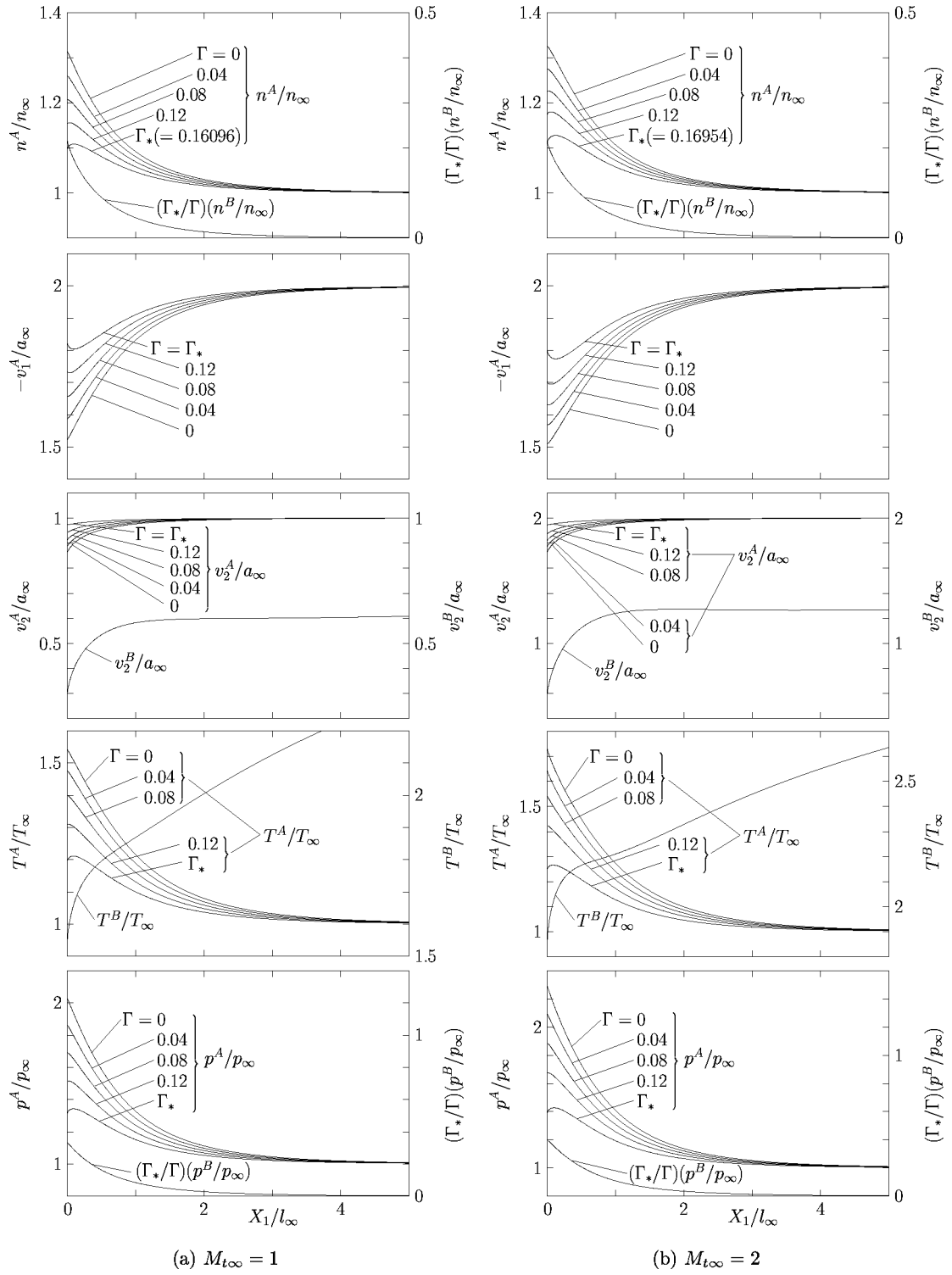

FIG. 6. Profiles of the macroscopic quantities for $M_{n\infty}=2$, $T_\infty/T_w=1$, and $p_\infty/p_0=4$. (a) $M_{t\infty}=1$ and (b) $M_{t\infty}=2$. See the caption of Fig. 5.

According to Ref. 4, the function $\hat{\mathcal{N}}_f$, along with the continuity equation in the Knudsen layer, is required as a part of the boundary condition for the Euler set of equations in the continuum limit. For this reason, we give some of the numerical data for $\hat{\mathcal{N}}_f$. Table III shows the data for $\hat{\mathcal{N}}_f$ in the case $T_\infty/T_w=1$. The data for $T_\infty/T_w=0.5$, 1.5, and 2 are given in Tables IX, XI, and XII in Ref. 20, respectively (Table X in Ref. 20 is the same as Table III here). Figure 8 shows $\hat{\mathcal{N}}_f$ versus $M_{t\infty}$ for various Γ and that versus Γ for various $M_{t\infty}$ in the case of $M_{n\infty}=1.2$, $T_\infty/T_w=1$, and $p_\infty/p_w=20$ [(a)] and of $M_{n\infty}=2$, $T_\infty/T_w=2$, and $p_\infty/p_w=10$ [(b)]. As is seen from Table III, the $\hat{\mathcal{N}}_f$ depends weakly on $M_{n\infty}$ and p_∞/p_w (see also Tables IX–XII in Ref. 20) and increases with $M_{t\infty}$ and Γ (see Fig. 8). The dependence on

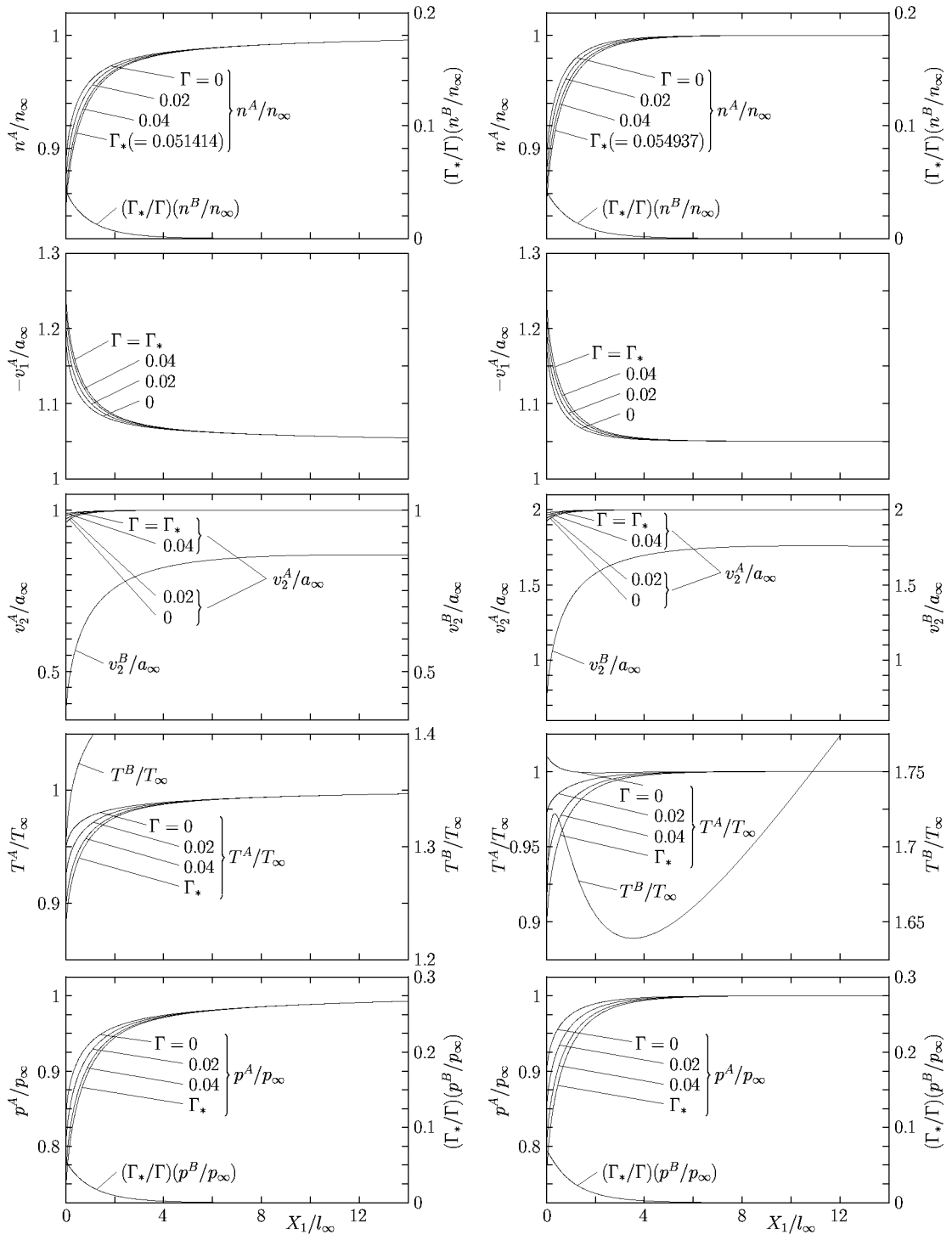

FIG. 7. Profiles of the macroscopic quantities for $M_{n\infty}=1.05$, $T_\infty/T_w=1$, and $p_\infty/p_0=22$. (a) $M_{t\infty}=1$ and (b) $M_{t\infty}=2$. See the caption of Fig. 5.

T_∞/T_w is also weak (see Tables IX–XII in Ref. 20).

If we denote by $\hat{\mathcal{N}}_{f*}$ the $\hat{\mathcal{N}}_f$ corresponding to $\hat{F}_*^B$, we have [see Eq. (31) in Ref. 2]

$$\hat{\mathcal{N}}_f=(\Gamma/\Gamma_*)\hat{\mathcal{N}}_{f*}. \tag{26}$$

Since $\hat{F}_*^B$ depends on $M_{n\infty}$, $M_{t\infty}$, T_∞/T_w, and p_∞/p_0, the quantity $\hat{\mathcal{N}}_{f*}$, as well as Γ_*, is a function of these four parameters. The data in Table III have been computed in the following way. We first solve p_∞/p_0 corresponding to the given set ($M_{n\infty}$, $M_{t\infty}$, T_∞/T_w, p_∞/p_w, Γ) from Eq. (12) with the help of interpolation based on the numerical data of $\Gamma_*(M_{n\infty},M_{t\infty},T_\infty/T_w,p_\infty/p_0)$. Next, we solve the half-space problem for the total mixture numerically to obtain $\hat{F}$ for the original values of $M_{n\infty}$, $M_{t\infty}$, and T_∞/T_w and the

TABLE III. $\hat{\mathcal{N}}_f(M_{n\infty}, M_{t\infty}, T_\infty/T_w, p_\infty/p_w, \Gamma)$ as a function of $M_{n\infty}$, $M_{t\infty}$, p_∞/p_w, and Γ ($T_\infty/T_w=1$). There is no solution for $\Gamma=0.1$ in the case $M_{n\infty}=1.2$ and $p_\infty/p_w=10$.

	$M_{n\infty}=1.2$									
	$p_\infty/p_w=10$					$p_\infty/p_w=20$				
$\Gamma\backslash M_{t\infty}$	0	0.4	1	1.5	2	0	0.4	1	1.5	2
0	0	0	0	0	0	0	0	0	0	0
0.0125	0	0.002 8903	0.007 3211	0.011 183	0.015 261	0	0.002 8131	0.007 1206	0.010 868	0.014 819
0.025	0	0.005 8193	0.014 740	0.022 516	0.030 724	0	0.005 6656	0.014 342	0.021 891	0.029 848
0.05	0	0.011 793	0.029 872	0.045 628	0.062 250	0	0.011 487	0.029 081	0.044 389	0.060 517
0.1						0	0.023 590	0.059 725	0.091 161	0.124 25
	$M_{n\infty}=1.5$									
	$p_\infty/p_w=10$					$p_\infty/p_w=20$				
$\Gamma\backslash M_{t\infty}$	0	0.4	1	1.5	2	0	0.4	1	1.5	2
0	0	0	0	0	0	0	0	0	0	0
0.025	0	0.005 2962	0.013 423	0.020 525	0.028 054	0	0.005 1723	0.013 100	0.020 015	0.027 332
0.05	0	0.010 740	0.027 223	0.041 626	0.056 886	0	0.010 499	0.026 597	0.040 643	0.055 506
0.1	0	0.022 055	0.055 901	0.085 467	0.116 75	0	0.021 589	0.054 699	0.083 590	0.114 14
0.2	0	0.046 362	0.117 49	0.179 57	0.245 14	0	0.045 440	0.115 12	0.175 88	0.240 00
	$M_{n\infty}=2$									
	$p_\infty/p_w=10$					$p_\infty/p_w=20$				
$\Gamma\backslash M_{t\infty}$	0	0.4	1	1.5	2	0	0.4	1	1.5	2
0	0	0	0	0	0	0	0	0	0	0
0.025	0	0.004 4024	0.011 159	0.017 073	0.023 370	0	0.004 2989	0.010 885	0.016 630	0.022 724
0.05	0	0.008 9626	0.022 726	0.034 785	0.047 634	0	0.008 7637	0.022 204	0.033 950	0.046 432
0.1	0	0.018 518	0.046 971	0.071 920	0.098 500	0	0.018 149	0.046 013	0.070 412	0.096 370
0.2	0	0.039 180	0.099 384	0.152 14	0.208 23	0	0.038 518	0.097 682	0.149 50	0.204 55
0.4	0	0.086 187	0.218 49	0.334 11	0.456 53	0	0.084 941	0.215 30	0.329 18	0.449 71

obtained value of p_∞/p_0. Then, we solve the linear problem for the noncondensable gas numerically to obtain $\hat{F}^B_*$, from which $\hat{\mathcal{N}}_{f*}$ is computed. The $\hat{\mathcal{N}}_f$ is obtained from Eq. (26). However, once we know the existence range (14a) and (14b), there is no merit to use the above indirect procedure. Therefore, in order to obtain the data given in Tables IX, XI, and XII in Ref. 20, we made use of a direct method, namely, we numerically solved the original boundary-value problem for $(\hat{F}^A, \hat{F}^B)$, rather than the problem for $(\hat{F}, \hat{F}^B)$, specifying the original parameters $(M_{n\infty}, M_{t\infty}, T_\infty/T_w, p_\infty/p_w, \Gamma)$ and computed $\hat{\mathcal{N}}_f$ directly.

V. CONCLUDING REMARKS

The present paper is the second part of the study of a flow of a vapor condensing onto a plane condensed phase at incidence in the case where a noncondensable gas is present near the condensed phase. The case of subsonic condensation, i.e., the case where the component of the flow velocity of the vapor perpendicular to the condensed phase at infinity is subsonic, is studied in the first part,[2] whereas the case of supersonic (and sonic) condensation is considered in the present paper. As in the first part[2] and in the earlier works,[1,3] we restricted ourselves to the case where the molecules of the vapor and those of the noncondensable gas are mechanically identical. Making use of the general features of the solution discussed in Ref. 2, we derived essential properties of the parameter range that admits a steady solution (Sec. III). Then, with the help of the property of the boundary of the parameter range discussed in Ref. 1 and extensive numerical computation based on the GSB model, the parameter range was constructed numerically (Sec. IV A). Finally, the behavior of the macroscopic quantities was clarified (Secs. IV B and IV C).

The present result for the parameter range that admits a solution, together with the corresponding result for subsonic condensation in Ref. 2, completes the boundary condition for the compressible Euler set of equations that describes the steady flows of the vapor around arbitrarily shaped condensed phases in the continuum limit in the presence of a tiny amount of the noncondensable gas.[4] The boundary condition, however, is still subject to the limitation that the vapor molecules are mechanically the same as the noncondensable-gas molecules and that the numerical results are obtained on the basis of the GSB model. The relaxation of these limitations would be an important future work.

ACKNOWLEDGMENTS

This work is supported by the Grants-in-Aid for the Scientific Research (Nos. 14350047 and 15760108) from the Japan Society for the Promotion of Science.

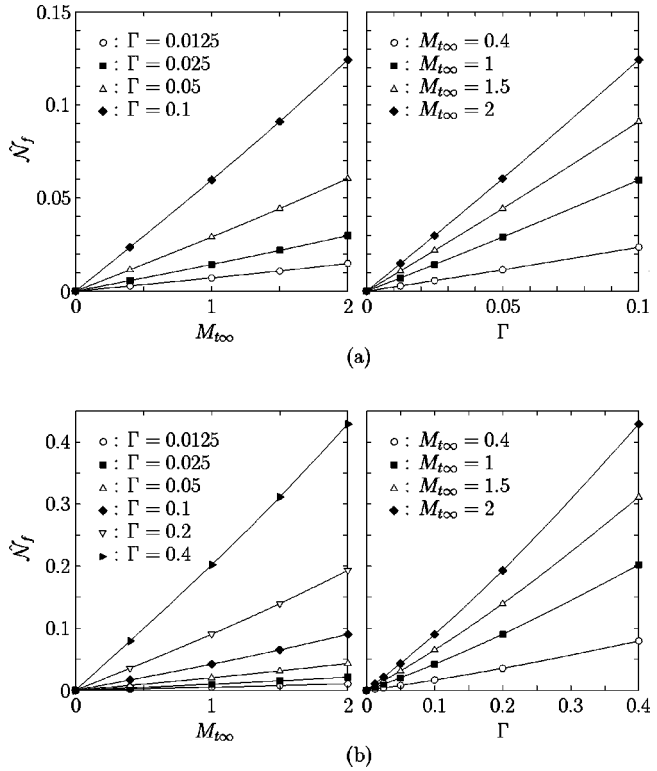

FIG. 8. $\hat{\mathcal{N}}_f(M_{n\infty}, M_{t\infty}, T_\infty/T_w, p_\infty/p_w, \Gamma)$ vs $M_{t\infty}$ for various Γ and that vs Γ for various $M_{t\infty}$. (a) $M_{n\infty}=1.2$, $T_\infty/T_w=1$, $p_\infty/p_w=20$; and (b) $M_{n\infty}=2$, $T_\infty/T_w=2$, $p_\infty/p_w=10$. The symbols ○, ■, △, ◆, ▽, and ▶ indicate the numerical data, which are connected by spline curves.

APPENDIX: DATA ON NUMERICAL COMPUTATION

In this appendix, we give some information on the accuracy of the present numerical analysis. In the present computation based on the GSB model collision term, we only need to handle two independent variables, $x_1[=(2/\sqrt{\pi})l_\infty^{-1}X_1]$ and ζ_1, because the transversal components ζ_2 and ζ_3 of the molecular velocity can be eliminated (see Sec. IV A of Ref. 2). The lattice systems for x_1 and ζ_1 used here are essentially the same as those used in Ref. 9 (see Appendix A of Ref. 9). In the present computation, however, the higher accuracy was attained by using wider computational regions, more lattice points, and smaller lattice intervals. The details of the lattice systems are omitted here.

We checked the accuracy of the computation in various ways. For many cases included in Tables I–IV in Ref. 20, we carried out computation with finer lattice systems with double lattice points either in x_1 or in ζ_1 and confirmed that the values of F_b and Γ_b in Tables I and II (and Tables I–VIII in Ref. 20) did not change. More specifically, concerning the x_1 lattices, this check was performed for all $M_{n\infty}$ and for $M_{t\infty}=0$ and 3 in the cases included in Tables I–IV in Ref. 20. The same check was also performed for many other cases in Tables I–IV in Ref. 20. As for the ζ_1 lattices, the check was performed for several cases for $M_{t\infty}=3$ of Tables I–VI in Ref. 20. In general, accurate computation becomes more difficult as $M_{t\infty}$ increases.

The conservation laws were also used for checking the accuracy. As in Ref. 2, let us introduce the following quantities:

$$(I_1, I_2, I_3, I_4)=\int \zeta_1(1, \zeta_1, \zeta_2, \zeta_j^2)\hat{F}\, d^3\zeta, \tag{A1}$$

$$I_1^B=\int \zeta_1\hat{F}^B\, d^3\zeta. \tag{A2}$$

The $n_\infty(2kT_\infty/m^A)^{1/2}I_1$, $2p_\infty I_2$, $2p_\infty I_3$, and $p_\infty(2kT_\infty/m^A)^{1/2}I_4$ indicate, respectively, the number of molecules, the X_1 component of the momentum, its X_2 component, and the energy of the total mixture transported in the positive X_1 direction across a unit area of the plane $X_1=$const per unit time; $n_\infty(2kT_\infty/m^A)^{1/2}I_1^B$ is the molecular flux of the noncondensable gas corresponding to $n_\infty(2kT_\infty/m^A)^{1/2}I_1$. It is shown in Appendix C of Ref. 2 that $I_1^B\equiv 0$ and that I_m ($m=1$, 2, 3, 4) are spatially uniform and are expressed in terms of the quantities at infinity as

$$\begin{aligned} &I_1=I_{1\infty}=-(5/6)^{1/2}M_{n\infty},\\ &I_2=I_{2\infty}=[(5/3)M_{n\infty}^2+1]/2,\\ &I_3=I_{3\infty}=-(5/6)M_{n\infty}M_{t\infty},\\ &I_4=I_{4\infty}=-(5/6)^{3/2}M_{n\infty}(M_{n\infty}^2+M_{t\infty}^2+3). \end{aligned} \tag{A3}$$

Because of numerical error, this uniformity is not satisfied exactly, and I_1^B does not vanish exactly. The deviations of the numerical values of $I_m-I_{m\infty}$ and I_{1*}^B from zero, where I_{1*}^B is the I_1^B with $\hat{F}^B=\hat{F}_*^B$ (see the third paragraph in Sec. III A), are estimated as follows:

$$\left.\begin{matrix}|(I_m-I_{m\infty})/I_{m\infty}|\\ |I_{1*}^B/I_{1\infty}|\end{matrix}\right\}<0.89\times 10^{-7}, \tag{A4}$$

for all $M_{n\infty}$, $M_{t\infty}$, and T_∞/T_w included in Tables I–IV in Ref. 20 ($M_{t\infty}=0$ is excluded for $m=3$ because $I_3=I_{3\infty}=0$ in this case).

[1] Y. Sone, K. Aoki, and T. Doi, "Kinetic theory analysis of gas flows condensing on a plane condensed phase: Case of a mixture of a vapor and a noncondensable gas," Transp. Theory Stat. Phys. **21**, 297 (1992).
[2] S. Taguchi, K. Aoki, and S. Takata, "Vapor flows condensing at incidence onto a plane condensed phase in the presence of a noncondensable gas. I. Subsonic condensation," Phys. Fluids **15**, 689 (2003).
[3] K. Aoki and T. Doi, "High-speed vapor flows condensing on a plane condensed phase in the presence of a noncondensable gas," in *Rarefied Gas Dynamics: Theory and Simulations*, edited by B. D. Shizgal and D. P. Weaver (AIAA, Washington, DC, 1994), p. 521.
[4] K. Aoki, S. Takata, and S. Taguchi, "Vapor flows with evaporation and condensation in the continuum limit: Effect of a trace of noncondensable gas," Eur. J. Mech. B/Fluids **22**, 51 (2003).
[5] V. Garzó, A. Santos, and J. J. Brey, "A kinetic model for a multicomponent gas," Phys. Fluids A **1**, 380 (1989).
[6] Y. Sone, "Kinetic theory of evaporation and condensation—Linear and nonlinear problems," J. Phys. Soc. Jpn. **45**, 315 (1978).
[7] Y. Sone, K. Aoki, and I. Yamashita, "A study of unsteady strong condensation on a plane condensed phase with special interest in formation of steady profile," in *Rarefied Gas Dynamics*, edited by V. Boffi and C. Cercignani (Teubner, Stuttgart, 1986), Vol. 2, p. 323.
[8] K. Aoki, Y. Sone, and T. Yamada, "Numerical analysis of gas flows condensing on its plane condensed phase on the basis of kinetic theory," Phys. Fluids A **2**, 1867 (1990).

[9]K. Aoki, K. Nishino, Y. Sone, and H. Sugimoto, ''Numerical analysis of steady flows of a gas condensing on or evaporating from its plane condensed phase on the basis of kinetic theory: Effect of gas motion along the condensed phase,'' Phys. Fluids A **3**, 2260 (1991).
[10]M. N. Kogan and A. A. Abramov, ''Direct simulation solution of the strong evaporation and condensation problem,'' in *Rarefied Gas Dynamics*, edited by A. E. Beylich (VCH, Weinheim, 1991), p. 1251.
[11]A. P. Kryukov, ''Strong subsonic and supersonic condensation on a plane surface,'' in *Rarefied Gas Dynamics*, edited by A. E. Beylich (VCH, Weinheim, 1991), p. 1278.
[12]Y. Sone, F. Golse, T. Ohwada, and T. Doi, ''Analytical study of transonic flows of a gas condensing onto its plane condensed phase on the basis of kinetic theory,'' Eur. J. Mech. B/Fluids **17**, 277 (1998).
[13]Y. Sone, ''Kinetic theoretical studies of the half-space problem of evaporation and condensation,'' Transp. Theory Stat. Phys. **29**, 227 (2000).
[14]Y. Sone, S. Takata, and F. Golse, ''Notes on the boundary conditions for fluid-dynamic equations on the interface of a gas and its condensed phase,'' Phys. Fluids **13**, 324 (2001).
[15]A. V. Bobylev, R. Grzhibovskis, and A. Heintz, ''Entropy inequalities for evaporation/condensation problem in rarefied gas dynamics,'' J. Stat. Phys. **102**, 1151 (2001).
[16]A. V. Gusarov and I. Smurov, ''Gas-dynamic boundary conditions of evaporation and condensation: Numerical analysis of the Knudsen layer,'' Phys. Fluids **14**, 4242 (2002).
[17]Y. Sone, *Kinetic Theory and Fluid Dynamics*, Modeling and Simulation in Science, Engineering and Technology (Birkhäuser, Boston, 2002).
[18]P. L. Bhatnagar, E. P. Gross, and M. Krook, ''A model for collision processes in gases. I. Small amplitude processes in charged and neutral one-component systems,'' Phys. Rev. **94**, 511 (1954).
[19]P. Welander, ''On the temperature jump in a rarefied gas,'' Ark. Fys. **7**, 507 (1954).
[20]See EPAPS Document No. E-PHFLE6-16-503401 for tables and figures. A direct link to this document may be found in the online article's HTML reference section. The document may also be reached via the EPAPS homepage (http://www.aip.org/pubservs/epaps.html) or from ftp.aip.org in the directory /epaps/. See the EPAPS homepage for more information.